10. Binary Pulsars to test General Relativity

10.1. Binary pulsars are rare systems.

After the discovery of the first pulsar in 1968 by Hewish and Bell the search and study of pulsars quickly became a new and growing research field taken up by nearly all large radioastronomy observatories. By 1972 already seven dozen pulsars were known, all discovered by examining strip-chart records which were soon replaced by computerized searches. It was obvious that pulsars are very precise clocks with extremely stable periods and slowdown rates of the order of $\dot{t}_P \approx 10^{-13} - 10^{-19}$. If a pulsar is accompanied by an equally compact companion, a white dwarf, a neutron star or a black hole (at a distance approximately Moon-Earth) such a system would offer an ideal laboratory to study effects in strong gravitational fields and to test General Relativity under strong field conditions. Today nearly 2000 pulsars are known in our galaxy, only about 4 % are in binary systems and most of those are ms-pulsars with a low mass companion. Mass and momentum transfer from the companion lead to a reloading of the pulsar. Such systems will further evolve into low mass X-ray binary systems (LMXB) with a fast spinning ms-pulsar ($t_P \approx 1 - 10\,ms$), see also lect. 09.

Binary pulsars with high mass companions (main sequence stars or neutron stars) are found to have eccentric orbits ($0{,}15 < e < 0{,}90$). If the mass of the companion is large enough to finally lead to a core supernova explosion a second NS will be born. In most cases the SN explosion would disrupt the binary system. The discharged NS will then travel with considerable peculiar velocity through the galaxy and will be observable for some time as singular pulsar. In some rare cases the binary system might be kept intact. Such a system is PSR 1913 +16, the binary pulsar discovered and observed by R.A. Hulse and J.H. Taylor, both honoured for their work with the Nobel prize in 1993. They used for most of their observations the 305-m-Radiotelescope at Arecibo in Puerto Rico.

PSR B1913+16 Observation data	**Companion**:
Epoch B1950.0 Equinox B1950.0 **Constellation** Aquila **Right ascension** $19^h\ 13^m\ 12.4655^s$ **Declination** 16° 01′ 08.189″ Astrometry **Distance** 21,000 ly (6400 pc) Details **Mass** 1.441 M_{sol} **Radius** 1.4×10^{-5} R_{sol} **Rotation** 59.02999792988 ms	• Mass of companion 1.387 M_{Sol} • Orbital period 7.751939106 hr • Eccentricity 0.617131 • Semimajor axis 1,950,100 km • Periastron separation 746,600 km • Apastron separation 3,153,600 km • Orbital velocity of stars at periastron (relative to center of mass) 450 km/sec • Orbital inclination ”i”= 45° • Change of periastron 4,2° per year • Decrease of semimajor axis 3,5 m per year

Table 10.1. Data from the binary pulsar PSR B1913+16 of Hulse and Taylor.

In April 2003 a team of the British Jodrell Bank Radio Observatory (M. Burgay, M. Kramer et al.) discovered the 22,8-ms pulsar J 0737–3039. They observed this system further with the Australian Parkes Radiotelescope. In October 2003 they detected radio signals from the second NS, a pulsar with a period of 2,8 s. Briefly said, up to the present this double pulsar

Fig. 10.1. The 305 m spherical reflector of the Arecibo Radio Telescope

Fig. 10.2. View of the beam steering mechanism. The wave lenth range of operation covers 3 cm – 1m.

is the most relativistic binary system ever discovered. At present the pair is understood as an old recycled 23 ms-pulsar and a young 2,8 s-pulsar orbiting around the common centre of mass in a slightly eccentric ellipse with surprisingly short period of 147 min. The inclination is nearly 90° which allows practically an edge-on observation. The masses are for Pulsar A $m_A = 1{,}3381 \pm 0{,}0007\, M_{sol}$ and for B $m_B = 1{,}2489 \pm 0{,}0007\, M_{sol}$. But before we discuss the results we will have a look at the measurements of pulsar timing to understand how the high accuracy has been achieved.

10.2. Pulsar timing.

The pulse shape may change slightly with time depending on the state of surrounding plasma. Individual pulses are usually weak and have a jitter in arrival time. Therefore one uses averaged profiles instead of individual pulses. For this purpose a window of timing is set given by the extend of the pulse profile. The profile from previous observations is used to construct a template with high signal to noise ratio. The time-offset between the template and the newly obtained profile determines the time of arrival (TOA) which is the key quantity of interest. Pulsar timing means counting the number N of NS rotations between two observations

$$N = N_0 + \nu_0 (t - t_0) + \frac{1}{2}\dot{\nu}(t - t_0)^2 + \frac{1}{6}\ddot{\nu}(t - t_0)^3 + \cdots \qquad (10.1)$$

N_0 and t_0 are "phase" and time of an arbitrary reference observation. It is important that the observed rotational phase N or the difference $N - N_0$ must always contain an integer number of rotations. The error of measurement σ may be a fraction of the pulsar period. The time of measurement Δt is usually some years, then the statistical error is quite small and decreases further with Δt. As an example take the error of TOA-measurements to be $\sigma = 6 \cdot 10^{-4}$ turn per second, the observation time $\Delta t = 25$ years, then the error in frequency will be

$$\delta\nu = \frac{\sigma_{TOA}}{\Delta t} = \frac{6\cdot 10^{-4}}{25\cdot 3{,}15\cdot 10^{7}} = 8\cdot 10^{-13}\ \text{Hertz} \qquad (10.2)$$

This example gives actually the precision of frequency for the original ms-pulsar B1937 + 21.

In order to determine relevant parameter of a pulsar system a considerable amount of corrections have to be applied to the original TOA-data. The pulses are measured at a radio observatory on Earth that is in a so called topocentric frame. This time can be corrected to the time in the solar system center of mass (the barycentric frame) assuming this to be nearly inertial and commoving with the pulsar. One has also to take into account the dispersion of radiowaves in the interstellar plasma which result in an effective index of refraction n changing the velocity of light as $c' = \frac{c}{n}$. The effect depends on the column density of free electrons which the radio wave passes on its way through the galaxy and gives an estimate of the pulsar's distance. When all effects due to the solar system have been corrected The delay

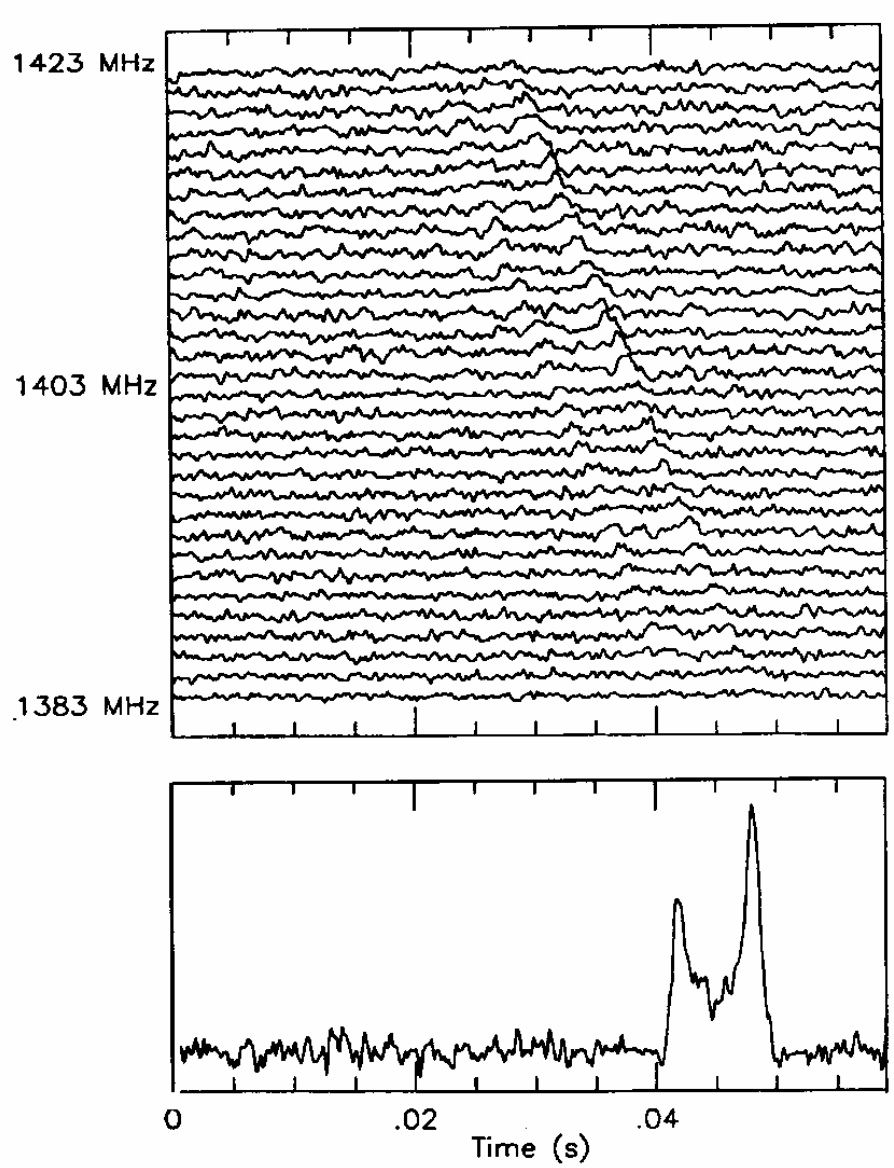

Fig. 10.3. The upper figure shows the dispersion (phase shift with frequency) of pulses , the lower figure the pulse profile from a 5 minute observation of PSR 1913+16 (J.A. Hulse Nobel lecture Dec. 1993).

concerning the pulsar binary system can be determined. Three different delays are distinguished:

Δ_R the Römer-delay considers the classical light travel across the orbit of the pulsar,

Δ_E the Einstein delay is the time delation from the moving pulsar and the gravitational redshift caused by the moving companion,

Δ_S the Shapiro delay accounts for the extra time required by the pulse when travelling through the curved space-time

When all these effects are correctly taken into account the timing residuals, which are the differences between the observed TOA and the predicted TOA, are weak and noisy signals without any periodic fraction (s. fig. 10.3. a). Errors in any of these parameters lead to very specific systematic signatures which are easily identified (s. fig. 10.3. b – d).

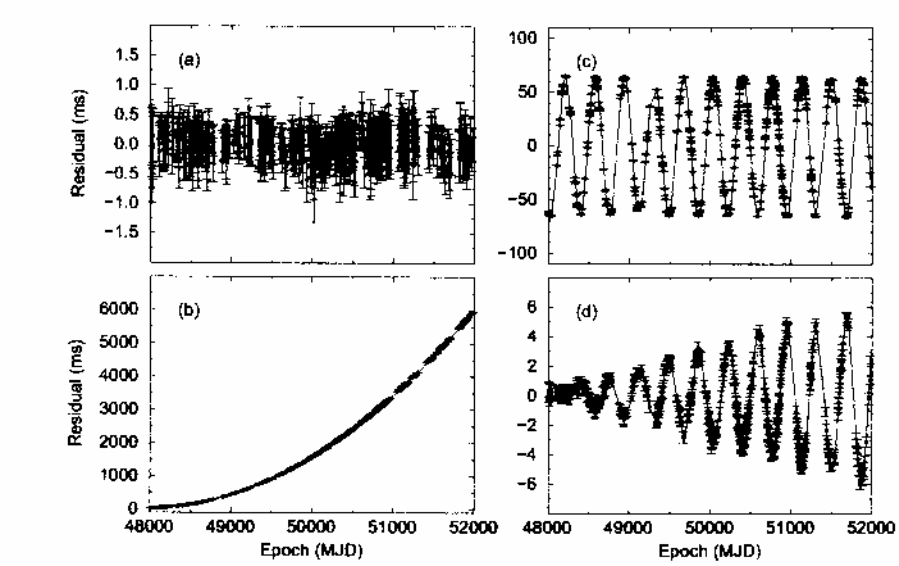

Fig. 10.4. a) The residual of a good timing solution and no unmodeled effects. c) indicates an error in position, b) shows an error in the frequency derivative $\dot{\nu}$, d) shows an unmodeled pulsar motion. (from Lorimer and Kramer, Handbook of Pulsar Astronomy, Cambridge 2005)

10.3. Binary orbits and its classical parameters.

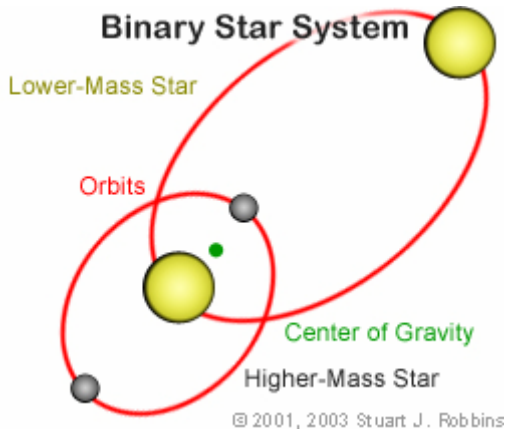

Fig. 10.5. Binary orbits

In a binary star system both components move around the common centre of mass. The line connecting both star must always go through the centre of mass. The shortest distance of the stars is called "periastron" distance fulfilled by the components in the figure at the left side near the centre of mass. The stars reach their largest distance in the "apastron" also shown in the figure. The two ellipses are in one plane

How many parameters are needed to uniquely define a binary system and predict the positions of the components for any time in the past or in the future? We need the following 8 elements:

1) position coordinates or ephemeredes in rectacension and declination
2) period P_b or time of one orbital motion
3) time of periastron passage
4) semimajor axis a but usually only $x = a \cdot \sin i$ is observed
5) e excentricity
6) the inclination of orbit i
7) the longitude of periastron ω
8) the position angle of the ascending node o

The angles i and o give the position of the orbital plane relative to the reference plane of the observer. In a pulsar binary the rotation periods, their time derivations and the pulse phase times should also be well known.

10.3. Post-Keplerian orbits.

In strong gravitational fields the orbits deviate from the classical Keplerian motion. It is known from classical mechanics that the r^{-1}-potential is the only one leading to closed circles or closed ellipses. We have already seen that the Schwarzschild metric adds a further r^{-2}-term to the effective potential. We therefore do not expect closed orbits. Instead the semimajor axis rotates slowly. In what follows only first order post-Newtonian corrections to the two-body motion is taken into account. As a justification consider the uncertainty of the TOA which is $\Delta t = 15\mu s$. This is of the same order of magnitude as the Schwarzschild radius of the pulsar which is $\frac{r_S}{c} \approx 7\mu s$. (We mentioned already that the actual precision obtained depends on the time of measurement expressed as number of pulses received). The second order corrections would lead to $\frac{r_S}{c}\left(\frac{\upsilon}{c}\right)^2 \approx 10^{-5}\mu s$

Fistly the advance of the periastron is expressed by

1) $\dot{\omega} = \frac{2\pi}{t_{Bin}} k$
2) γ is a relativistic time delation and redshift parameter
3) $\frac{d}{dt} P_b$ is a secular change of the orbit period. This is possible when the system looses energy. This is actually predicted by GR: the energy especially of short period binaries is radiated away by gravitational radiation.
4) $\Delta_S = \Delta t_S = \int_{source}^{observer} dr$ is the Shapiro time delay caused by the curvature od space-time near the pulsar. See fig.10.9 for an illustration.

The post-Keplerian quantities can be expressed as functions of the Keplerian parameters which will be given here in the framework of the GR (this is however possible in any gravitational theory). We find

$$\dot{\omega} = 3\left(\frac{2\pi}{P_b}\right)^{5/3} (T_{\odot} M)^{2/3} (1-e^2)^{-1} \tag{10.3}$$

$$\gamma = e\left(\frac{P_b}{2\pi}\right)^{1/3} T_{\odot}^{2/3} M^{-4/3} m_2 \cdot (m_1 + 2m_2) \tag{10.4}$$

$$\frac{dP_b}{dt} = -\frac{192\pi}{5}\left(\frac{2\pi}{P_b}\right)^{5/3}\left(1+\frac{73}{24}e^2+\frac{37}{96}e^4\right)(1-e^2)^{-7/2} T_{\odot}^{5/3} m_1 \cdot m_2 M^{-1/3} \tag{10.5}$$

where

$$M = m_1 + m_2 \text{ and } T_{\odot} = \frac{GM_{sol}}{c^3}$$

$T_{\odot}$ is the time of light to cross the Schwarzschild radius of the sun.

$$s = \sin i = x\left(\frac{2\pi}{P_b}\right)^{2/3} T_{\odot}^{-1/3} M^{2/3} m_2^{-1} \tag{10.6}$$

with $x = \dfrac{a_1 \sin i}{c}$

$$\Omega_{SO,2} = T_{\odot}^{2/3}\left(\frac{2\pi}{P_b}\right)^{5/3} \cdot \frac{1}{1-e^2}\frac{m_1(4m_2+3m_1)}{2(m_1+m_2)^{4/3}} \tag{10.7}$$

$$\Delta_S = -\frac{r_S}{c}\ln\left[1-\vec{s}(OS)\cdot\vec{s}(OM)\right] \tag{10.8}$$

is the Shapiro delay. Here r_S is the Schwarzschild radius of the gravitating mass, $\vec{s}(OS)$ is the unit vector pointing from the observer to the source (the pulsar) and $\vec{s}(OM)$ the unit vector from observer to the gravitating mass.

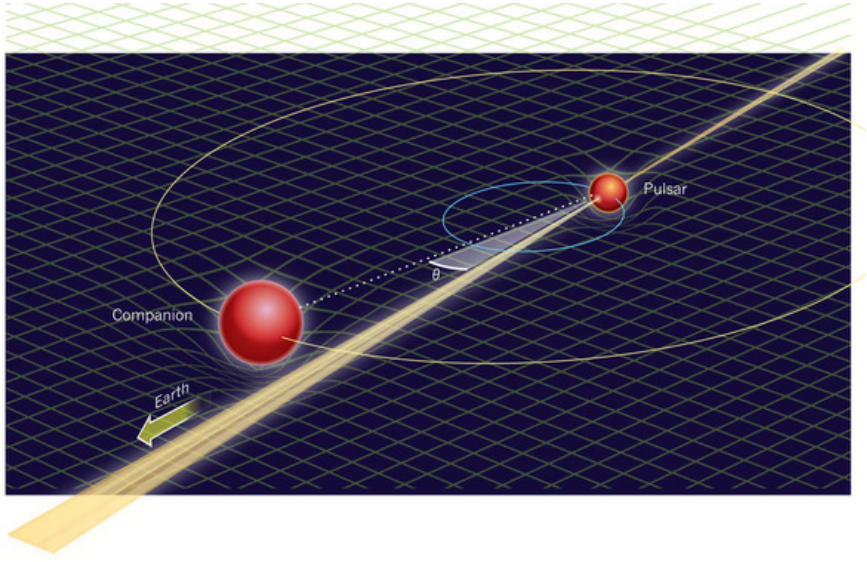

Fig. 10.6. The Shapiro delay in the view of an artist. Credit: M.Coleman Miller.

10.4. Determination of the parameters from the data.

All post-Keplerian parameter are functions of the two masses m_1 and m_2. Therefore each of them gives a curve in a m_1-m_2-plot. If the theory of gravitation is consistent all curves should meet in one point. Below are two mass-mass diagrams, fig. 10.7 with the data of PSR B1913+16, the Hulse-Taylor system, fig. 10.8 with the data of the double pulsar J0737-3039.

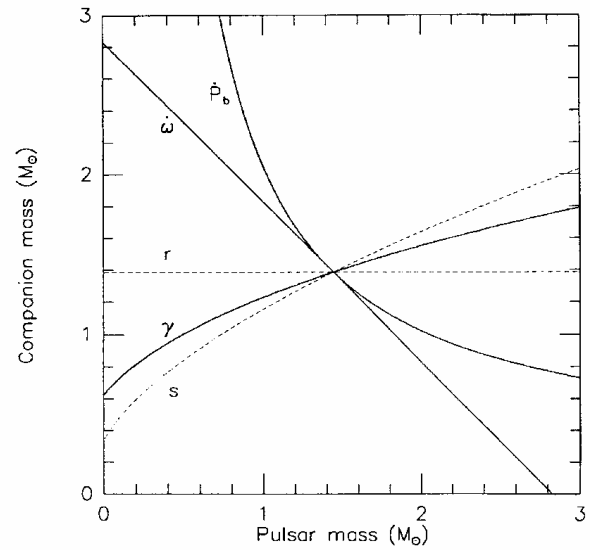

Fig. 10.7. PSR B1913+16 observational data: Three post-Newtonian parameter $\dot{P}_b$, $\dot{\omega}$, γ and $s = \sin i$ (dashed line, added later) are presented in a mass-mass-plot. They meet within the experimental error of 0,35% in one point which indicates the consistence of the applied gravitational theory,
i.e. GR including gravitational waves.

At least two curves are necessary to determine the masses m_1 and m_2. If this has been accomplished any further curve gives one more post-Keplerian parameter, that is one more test of GR. The Hulse-Taylor binary pulsar allowed to determine 3 post-Newtonian parameter:

the inclination $s = \sin i$, the change of periastron (4,2° per year) and the decrease of the semimajor axis (3,5 m per year). In the case of the new double pulsar **J0737-3039** the determination of 5 post-Keplerian parameter have been achieved. It is expected that it will become possible to determine even more parameter with growing observation time. This concerns especially the relativistic spin-orbit coupling. Since the orbital momentum is much larger than the spin momentum we may speak of the pulsar spin precession about the orbital momentum axis which has the direction of the orbital plane (geodetic precession). This effect should also be observable as a change of the pulse profile since the direction of the emission cone changes with precession. No such effect was observed with Pulsar A indicating only a small misalignment of spin and orbital momentum. Luckily pulsar B already shows this effect. Furthermore a 30s-eclipse of A was observed created by the blocking of the rotating magnetosphere of B which could be correctly described by a geometric model. From this fitting it was possible to derive a preliminary value for the rate of change of the azimutal spin position $\Omega_{SO,B} = 4{,}77 \pm 0{,}66\ yr^{-1}$. One expects also a change of the orientation of the binary orbit which is proportional to the pulsar's and the companion's spin moment. Both contain the moment of inertia which otherwise cannot easily be determined from observation.

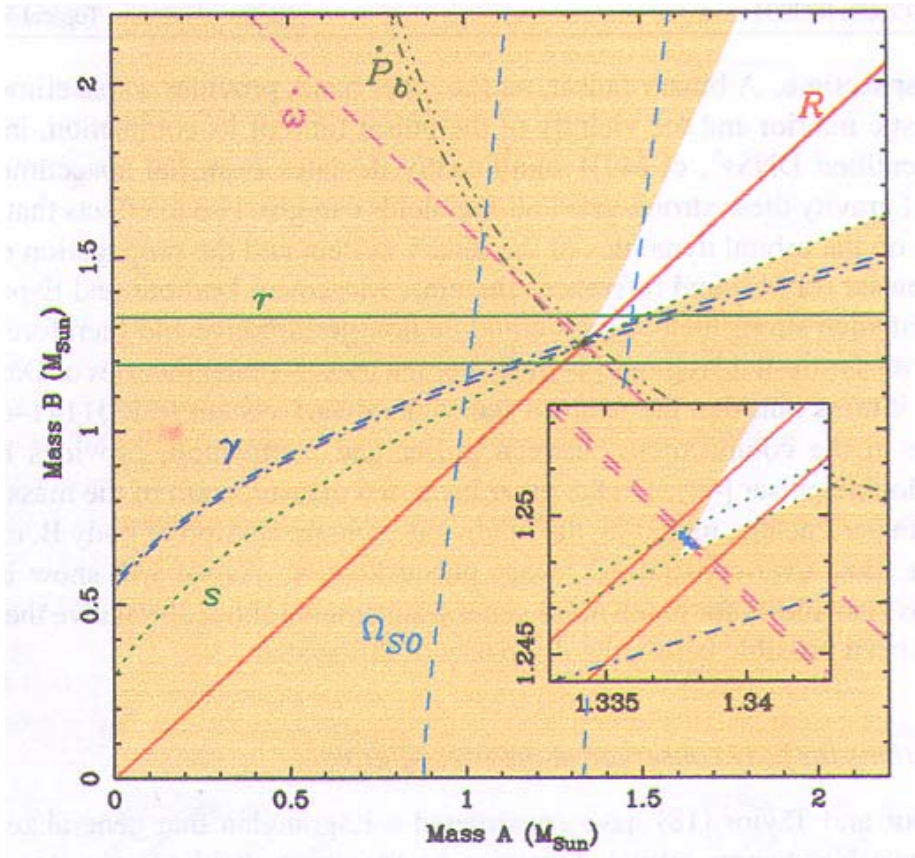

Fig. 10.8. Mass-mass diagram of J0737-3039. The uncertainties are smaller than the width of the lines. Each pair of lines enclose the 68% confidence range of the respective quantity. $\dot{P}_b$ is the decline of orbital period, $\dot{\omega}$ advance of periastron, γ the redshift. The red line is the plot of $R = m_A / m_B$, *r* means Shapiro parameter, s inclination and Ω_{SO} rel. spin-orbit coupling(s. M. Kramer and N. Wex)

Table 1. Astrometric and system parameters of the double pulsar. Quantities for which a single entry is given for both A and B were determined from timing of pulsar A. See [9] for more details. Measured post-Keplerian (PK) parameters are listed in table 2.

System parameters	PSR J0737–3039A	PSR J0737–3039B
Spin frequency ν (Hz)	44.054 069 392 744(2)	0.360 560 355 06(1)
Spin frequency derivative $\dot{\nu}$ (s^{-2})	$-3.4156(1) \times 10^{-15}$	$-0.116(1) \times 10^{-15}$
Right ascension α	$07^h37^m51\overset{s}{.}324927(3)$	
Declination δ	$-30°39'40\overset{''}{.}7195(5)$	
Proper motion in RA (mas yr^{-1})	−3.3(4)	
Proper motion in declination (mas yr^{-1})	2.6(5)	
Total proper motion (mas yr^{-1})	4.2(4)	
Distance (pc)[a]	1150(−160, +220)	
Orbital period P_b (day)	0.102 251 562 48(5)	
Eccentricity e	0.087 777 5(9)	
Orbital inclination angle (deg)[b]	88.69(−76, +50)	
Total system mass ($M_\odot$)[b]	2.58708(16)	
Mass ratio, R	1.0714(11)	
Projected semi-major axis $x = (a/c) \sin i$ (s)	1.415 032(1)	1.516 1(16)
Neutron star mass ($m_\odot$)[b]	1.3381(7)	1.2489(7)

[a] Derived from very long-baseline interferometry [11].
[b] Derived using measurements of PK parameters (see section 3 and table 2).

Table 10.2. (s. M. Kramer and N. Wex)

Table 2. Post-Keplerian (PK) parameters measured for the double pulsar and their comparison with expectations from general relativity (GR). These expectations were derived for the masses as determined from the theory-independent mass ratio and the most precisely measured PK parameter $\dot{\omega}$. For measurement details of the first 5 PK parameters, see [9], and consult [19] for the last one.

PK parameter	Observed	GR expectation	Ratio
$\dot{\omega}$ (deg yr^{-1})	16.899 47(68)	–	–
$\dot{P}_b$	1.252(17)	1.24787(13)	1.003(14)
γ_A (ms)	0.3856(26)	0.38418(22)	1.0036(68)
s	0.999 74(−39, +16)	0.999 87(−48, +13)	0.999 87(50)
r_A (μs)	6.21(33)	6.153(26)	1.009(55)
$\Omega_{SO,B}$ (deg yr^{-1})	4.77(+0.66, −0.65)	5.0734(7)	0.94(13)

Table 10.3. (s. M. Kramer and N. Wex)

In particular the calculated values depend on the used equation of state of neutron matter, a further motivation to improve the accuracy of the determination of spin-orbit effects.
From this fitting it was possible to derive a preliminary value for the rate of change of the azimutal spin position $\Omega_{SO,B} = 4{,}77 \pm 0{,}66\ yr^{-1}$. In particular the calculated values depend on the used equation of state of neutron matter, a further motivation to improve the accuracy of the determination of spin-orbit effects.

We have seen that Einstein's theory of gravitation, known as Theory of General Relativity, has smoothly passed all five tests provided by the double pulsar system J0737-3039. There still remains the question if all alternative theories of gravity with these tests are safely excluded. This question was further discussed by M. Kramer and N. Wex in Class. Quantum Grav. 26 (2009) 073001. Several known alternative approaches have been analyzed und could be eliminated.

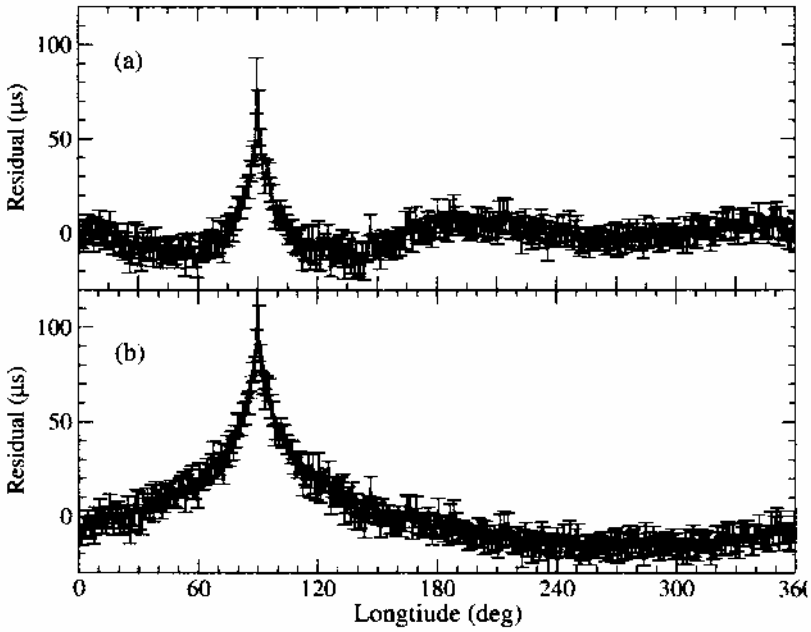

Fig. 10.9. The Shapiro delay caused by the gravitational potential of B seen in the timing residuals of A. The full line shows the predicted delay at the center of the data span. The residuals were averaged in 1° bins of longitude.

On the other hand the double pulsar is the most over-constrained binary pulsar system known which allows for more general statements about alternative theories. The interested student will find further discussion of these questions in the paper of Kramer and Wex including references.

10.5. Problems.

10.5.1. Estimate the Shapiro delay of the pulses from pulsar A caused by the gravitational potential of B (s. Fig. 10.6). The pulsar beam of A passes B at a minimum distance of ca. 30 000 km (≈ 0,100 s). The inclination angle is i = 88,69°. The semi-major axis of A is $a_A / c = 1{,}415s$, the mass of B 1,25 *Msol.*

10.5.2. The components of the double pulsar move with a mean orbital speed of 300 km/s. The orbital plane is oriented parallel to the line of sight. Calculate the Doppler effect as time delay or advance. For simplicity assume a circular orbit. Note that the relativistic Doppler is

$$\Delta t' = \Delta t \cdot \frac{1 \pm \frac{\upsilon}{c}}{\sqrt{1 - \frac{\upsilon^2}{c^2}}}$$ Take account of the relativistic effect up to second order.

10.5.3. The components of the "double pulsar" have the pulse periods A 23 ms and B 2,8 s. Which of them is considered to be the older one and why?

References.

J.H. Taylor: Binary pulsars and relativistic gravity. Nobel lecture Dec. 8, 1993.
M. Kramer: The Double Pulsar. Seminaire Poincaré (2006) 63- 89.
M. Kramer and N. Wex: The double pulsar system: a unique laboratory for gravity. Class. Quantum Grav. 26 (2009) 073001
A. Lyne and M. Kramer: Gravitational labs in the sky. Physics World March 2005 p. 29
G. Esposito-Farése: Tests of Alternative Theories of Gravity.
33rd SLAC Summer Institute on Particle Physics (SSI 2005), 25 July - 5 August 2005. T025 1